PHYSICAL REVIEW A **73**, 051603(R) (2006)

# Mean-field phase diagrams of imbalanced Fermi gases near a Feshbach resonance

Hui Hu[1,2] and Xia-Ji Liu[2]
[1]*Department of Physics, Renmin University of China, Beijing 100872, China*
[2]*ARC Centre of Excellence for Quantum-Atom Optics, Department of Physics, University of Queensland, Brisbane, Queensland 4072, Australia*
(Received 13 March 2006; published 22 May 2006)

We propose phase diagrams for an imbalanced (unequal number of atoms or Fermi surface in two pairing hyperfine states) gas of atomic fermions near a broad Feshbach resonance using mean-field theory. Particularly, in the plane of interaction and polarization we determine the region for a mixed phase composed of normal and superfluid components. We compare our prediction of phase boundaries with the recent measurement and find a good qualitative agreement.

DOI: 10.1103/PhysRevA.73.051603 PACS number(s): 03.75.Hh, 03.75.Ss, 05.30.Fk

Two recent experimental studies of fermionic superfluidity in strongly interacting atomic $^6$Li gases with controlled population imbalance in two spin components have attracted intense interest from physicists in wide communities [1,2]. A very salient reason is the mysterious nature of the pairing mechanism [3–11]. Since the Bardeen-Cooper-Schrieffer (BCS) pairing requires an equal number of atoms in each spin state, the presence of spin population imbalance leads to some exotic forms of pairing, such as the finite-momentum paired Fulde-Ferrell-Larkin-Ovchinnikov (FFLO) state [3], the breached pairing or Sarma superfluidity [4,5], and phase separation [6]. However, the true ground state of imbalanced fermionic superfluidity remains elusive and has been the subject of debate for decades. The two recent experimental observations open up the intriguing possibilities for resolving this long-standing problem. As the population imbalance increases, the disappearance of superfluidity has been identified [1], and the phase separation of a unitary gas in trap has been observed [2].

Motivated by the significant experimental development, in this paper we present a general mean-field analysis of the ground state of homogeneous imbalanced atomic gases, focusing on the strongly interacting region near the broad Feshbach resonance, namely, the so-called crossover from BCS superfluidty to the Bose-Einstein condensation (BEC). Our goal is to map out the *qualitative* zero-temperature phase diagrams in the entire BCS-BEC crossover. A previous discussion of such phase diagrams is based on a purely educated guess [7]. A further analytic mean-field estimate is restricted to the narrow Feshbach resonance [8], for which the most fascinating crossover region has been essentially ruled out, and thus is of less experimental relevance.

In contrast to these prior theoretical studies, our analysis is in close connection to the experiment and has more predictive powers. Our main results may be summarized as follows. (1) Aside from the ability to include the exotic phases mentioned earlier, our mean-field calculation predicts a new phase (the saddle point solution below), which becomes energetically favorable for a finite population imbalance. However, the new solution is inherently unstable towards phase separation, signifying an inhomogeneous mixed phase. Around the crossover, consistent with the experimental observations [1,2], we find that the phase separation phase becomes dominant in the phase diagram. (2) We construct the phase boundary of superfluid-to-normal transitions, and compare it with the measurement by Zwierlein *et al.* [1]. The agreement is qualitatively good.

We consider an imbalanced Fermi gas of $^6$Li atoms across a broad Feshbach resonance, which is well described by using a single-channel model [12],

$$\mathcal{H} = \sum_{\mathbf{k}\sigma} \xi_{\mathbf{k}\sigma} c^\dagger_{\mathbf{k}\sigma} c_{\mathbf{k}\sigma} + g \sum_{\mathbf{k}\mathbf{k}'\mathbf{p}} c^\dagger_{\mathbf{k}\uparrow} c^\dagger_{\mathbf{p}-\mathbf{k}\downarrow} c_{\mathbf{p}-\mathbf{k}'\downarrow} c_{\mathbf{k}'\uparrow}. \tag{1}$$

Here the pseudospins $\sigma=\uparrow,\downarrow$ denote the two hyperfine states of $^6$Li, and $c^\dagger_{\mathbf{k}\sigma}$ is the fermionic creation operator with the kinetic energy $\xi_{\mathbf{k}\sigma}=\epsilon_{\mathbf{k}}-\mu_\sigma$ and $\epsilon_{\mathbf{k}}=\hbar^2\mathbf{k}^2/2m$. The chemical potentials are different, i.e., $\mu_{\uparrow,\downarrow}=\mu\pm\delta\mu$, to account for the population imbalance $\delta n=n_\uparrow-n_\downarrow$. $g$ is the bare interaction strength, and is expressed in terms of $s$-wave scattering length $a$ via $(4\pi\hbar^2 a/m)^{-1}=g^{-1}+\Sigma_{\mathbf{k}}(2\epsilon_{\mathbf{k}})^{-1}$.

In the mean-field approximation we decouple the interaction term by introducing an order parameter of Cooper pairs in momentum space $\Delta=-g\Sigma_{\mathbf{k}}\langle c_{\mathbf{q}/2-\mathbf{k}\downarrow} c_{\mathbf{q}/2+\mathbf{k}\uparrow}\rangle$, where the pairs may possess a nonzero center-of-mass momentum $\mathbf{q}$ in the case of spatially modulated states [13]. As a result, the order parameter in real space aquires a one-wave oscillation form: $\Delta(\mathbf{x})=-g\langle c_\downarrow(\mathbf{x}) c_\uparrow(\mathbf{x})\rangle=\Delta e^{i\mathbf{q}\cdot\mathbf{x}}$. The value of $q$, together with $\Delta$, are to be determined. The Hamiltonian can then be approximated by

$$\mathcal{H} = \sum_{\mathbf{k}\sigma} \xi_{\mathbf{k}\sigma} c^\dagger_{\mathbf{k}\sigma} c_{\mathbf{k}\sigma} - \Delta \sum_{\mathbf{k}} [c_{(\mathbf{q}/2)-\mathbf{k}\downarrow} c_{(\mathbf{q}/2)+\mathbf{k}\uparrow} + \text{H.c.}] - \frac{\Delta^2}{g},$$

$$= \sum_{\mathbf{k}} \psi^\dagger_{\mathbf{k}} [\xi_{\mathbf{k}+}\sigma_z + \xi_{\mathbf{k}-} - \Delta\sigma_x]\psi_{\mathbf{k}} + \mathcal{E}_0, \tag{2}$$

where in the second line we define a Nambu creation field operator: $\psi^\dagger_{\mathbf{k}}=(c^\dagger_{\mathbf{q}/2+\mathbf{k}\uparrow}, c_{\mathbf{q}/2-\mathbf{k}\downarrow})$, $\sigma_x$ and $\sigma_z$ are the $2\times 2$ Pauli matrices, $\xi_{\mathbf{k}\pm}=(\xi_{\mathbf{q}/2+\mathbf{k}\uparrow}\pm\xi_{\mathbf{q}/2-\mathbf{k}\downarrow})/2$, and $\mathcal{E}_0=\Sigma_{\mathbf{k}}(\xi_{\mathbf{k}+}-\xi_{\mathbf{k}-})-\Delta^2/g$. The above pairing Hamiltonian may be solved by the standard Bogoliubov transformation, or more straightforwardly, by employing the Nambu propagator $\mathbf{G}(\mathbf{k}, i\omega_m)=1/[(i\omega_m-\xi_{\mathbf{k}-})-\xi_{\mathbf{k}+}\sigma_z+\Delta\sigma_x]$ with quasiparticle energies $E_{\mathbf{k}\pm}=(\xi^2_{\mathbf{k}+}+\Delta^2)^{1/2}\pm\xi_{\mathbf{k}-}$. Here $\omega_m=(2m+1)\pi/\beta$ and $\beta=1/k_BT$. The thermodynamic potential thus takes the form

 

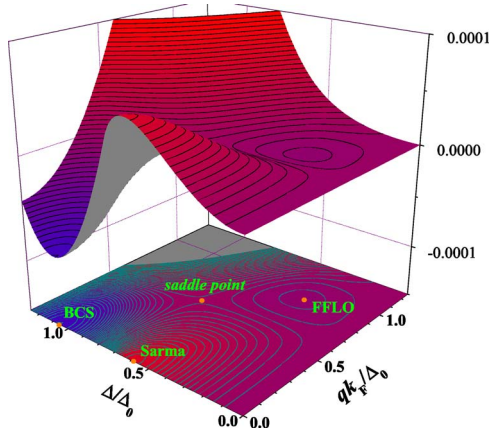


FIG. 1. (Color online) Landscape of the thermodynamic potential at $1/k_F a=-1$. The chemical potential is fixed to $\mu=0.98942\epsilon_F$. The competing ground states are (i) a normal Fermi gas with $\Delta=0$, (ii) a fully paired BCS superfluid with $\Delta=\Delta_0$, $q=0$, and $\delta n=0$, (iii) a breached pairing or Sarma superfluid with $\Delta<\Delta_0$, $q=0$, and $\delta n\neq 0$, (iv) a finite momentum paired FFLO superfluid with $\Delta<\Delta_0$, $q\neq 0$, and $\delta n\neq 0$, and (v) a saddle point phase intervening between the local BCS and FFLO minima.

$$\Omega=\frac{1}{\beta}\sum_{\mathbf{k}m}\mathrm{Tr}\ln\mathbf{G}(\mathbf{k},i\omega_m)+\mathcal{E}_0,$$

$$=-\frac{m\Delta^2}{4\pi\hbar^2 a}+\sum_{\mathbf{k}}\left[\xi_{\mathbf{k}+}-(\xi_{\mathbf{k}+}^2+\Delta^2)^{1/2}+\frac{\Delta^2}{2\epsilon_{\mathbf{k}}}\right]$$

$$+\frac{1}{\beta}\sum_{\mathbf{k}}[\ln f(-E_{\mathbf{k}+})+\ln f(-E_{\mathbf{k}-})],\qquad(3)$$

where $f(x)=[\exp(\beta x)+1]^{-1}$ is the Fermi distribution function. We shall confine ourselves to zero temperature, where the last term in $\Omega$ reduces to $\Sigma_{\mathbf{k}}[E_{\mathbf{k}+}\Theta(-E_{\mathbf{k}+})+E_{\mathbf{k}-}\Theta(-E_{\mathbf{k}-})]$.

The mean-field treatment presented above provides a simplest unified description for the uniform and spatially modulated superfluids. All these phases have to be determined using the stationary (*saddle point*) conditions: $\partial\Omega/\partial\Delta=0$, $\partial\Omega/\partial q=0$, as well as the requirement of number conservation $n=n_\uparrow+n_\downarrow=-\partial\Omega/\partial\mu$.

We now discuss separately the phase diagram in the situations where either the field $\delta\mu$ or the population imbalance $\delta n=-\partial\Omega/\partial\delta\mu$ is kept fixed. To this end, we trace the evolution of all available mean-field solutions with increasing the dimensionless coupling constant $\eta=1/k_F a$, where $k_F=(3\pi^2 n)^{1/3}$ is the noninteracting Fermi wave vector, and seek the one with the lowest energy (not the thermodynamic potential). To gain a physical insight into the competing ground states, we show in Fig. 1 the landscape of $\Omega$ at a selected set of parameters. At $\mathbf{q}=\mathbf{0}$ there is a Sarma solution situated between the trivial normal state at $\Delta=0$ and the local BCS minimum $\Delta_0$ and corresponding to a maximum of $\Omega$ as a function of $\Delta$. On the other hand, for large enough field mismatch, a spatially modulated pairing (known as FFLO phase) is driven with $\mathbf{q}\cdot\mathbf{k}_F\sim\delta\mu$. This forms another

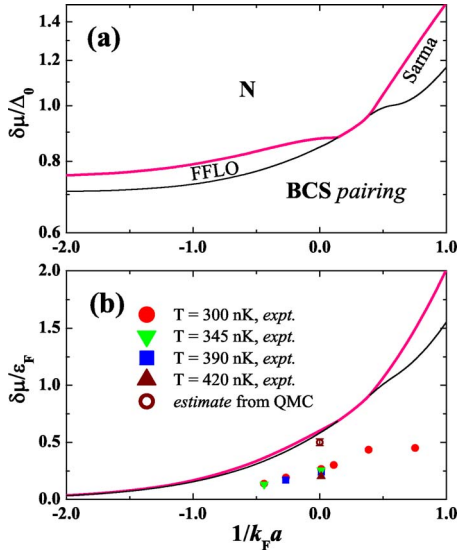


FIG. 2. (Color online) Phase diagram in the plane of interaction and chemical potential difference.

local minimum in the landscape. Interestingly, a saddle point solution necessarily emerges in order to separate the local BCS and FFLO minima.

It is worth noting that not all the solutions are stable. In the following we mainly focus on the stability against phase separation by the criterion $\partial\delta n/\partial\delta\mu>0$, which indicates the formation of an inhomogeneous mixed state. Another stability criterion that the superfluid density must be positive could also be readily examined [5].

*Fixed chemical potential difference*. We present in Fig. 2(a) the interaction-field phase diagram, constructed by finding out the state with the lowest free energy $F=\Omega+\mu n$. The general structure of the phase diagram can be understood by considering the BCS and BEC limits first. In the BCS limit with infinitely small attraction, $\eta\to-\infty$, the kinetic energy dominates and the Cooper pair formation is limited to the two Fermi surface. For $\delta\mu<\delta\mu_1=1/\sqrt{2}\Delta_0$, the ground state remains the BCS state. For $\delta\mu_1<\delta\mu<\delta\mu_2\simeq 0.754\Delta_0$, the Fermi surfaces may be translationally deformed, in order to increase the overlap for pairing. A FFLO state with spatially varying order parameter is therefore preferable. The transition from BCS to FFLO states is of first order. Finally, for $\delta\mu>\delta\mu_2$, the system translates continuously into a normal Fermi liquid phase. As an example, for $\eta=-1$ we show in Fig. 3(a) the numerical comparison of free energies of various competing states.

The ground state in the BEC limit of $\eta\to+\infty$ is also known on physical grounds. Because of the strong attraction, all the spin down fermions are likely to pair up with atoms in the other state, to form a condensate of tightly bounded objects in real space. The distortion of Fermi surfaces is prohibited, and then the leftover possibilities are the BCS pairing and the Sarma state, as confirmed numerically in Fig. 3(c). The latter state, in this strong coupling limit, is a *coherent* mixture of condensate and a remaining Fermi sea of unpaired atoms. It is energetically favorable only for $\delta\mu\simeq\epsilon_b$ as to create an unbound fermion, where $\epsilon_b=\hbar^2/2ma^2$ is the two-body binding energy. For sufficiently large mismatch

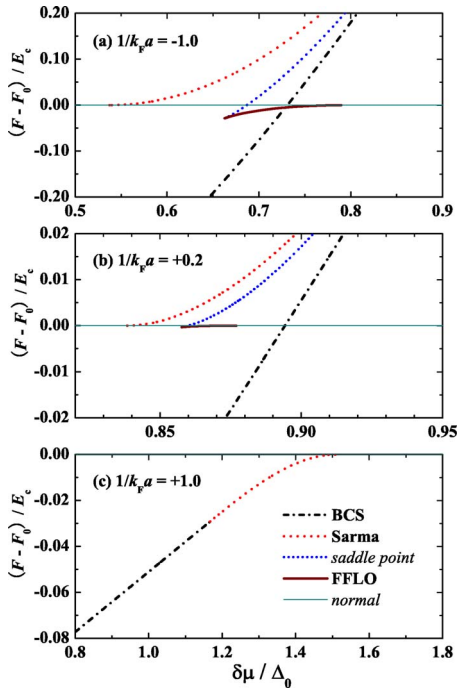


FIG. 3. (Color online) Comparison of free energies of available mean-field solutions at coupling constants as indicated, with the free energy of the normal gas $F_0$ being subtracted. $E_c = \mathcal{N}(0)\Delta_{BCS}^2/2$ is the condensation energy for a symmetric Fermi gas, $\mathcal{N}(0) = mk_F/(2\pi^2\hbar^2)$ is the density of state at the Fermi surface and $\Delta_{BCS} = 8\exp[\pi/(2k_Fa) - 2]$.

$\delta\mu \simeq \epsilon_b + 2^{2/3}\epsilon_F$, the condensate disappears and the gas becomes completely polarized. Transitions among BCS, Sarma, and normal phases are continuous.

The phase diagram in the two limits therefore are entirely different. Around the BCS-BEC crossover one could image a qualitatively change. In particular, the spatially varying FFLO and saddle point phases should cease to exist with increasing the coupling. We find numerically [i.e., see Fig. 3(b)] that for $0.15 < \eta < 0.40$ the system goes from BCS to the normal state, without experiencing the FFLO or the Sarma phase. Our mean-field finding is in sharp contrast with a previous proposal in Ref. [7], where a direct transition from FFLO to Sarma phase is anticipated. This anticipation is another topological possibility to connect the two limits.

In Fig. 2(b), by reexpressing $\delta\mu$ in terms of the noninteracting Fermi energy, we compare our results of the critical $\delta\mu$ for superfluid-to-normal transitions with the quantum Monte Carlo estimate [9] and the recent experimental data on the critical Fermi energy difference $(\delta E_F/\epsilon_F)_c$ [1]. These differences are calculated assuming a noninteracting dispersion: $(\delta E_F/\epsilon_F)_c = \{[1 + (\delta n/n)_c]^{1/3} - [1 - (\delta n/n)_c]^{1/3}\}/2$, where $(\delta n/n)_c$ is the measured critical population imbalance (see, i.e., Fig. 5 in Ref. [1]). The mean-field prediction is in good agreement with the Monte Carlo result, but is about two times larger than the measurement. This discrepancy should not be taken seriously since the mean-field theory is only qualitatively valid. On the other hand, only in the weakly coupling BCS regime do the chemical potentials equal the Fermi energies. Further, a quantitative comparison would require the consideration of the external trap.

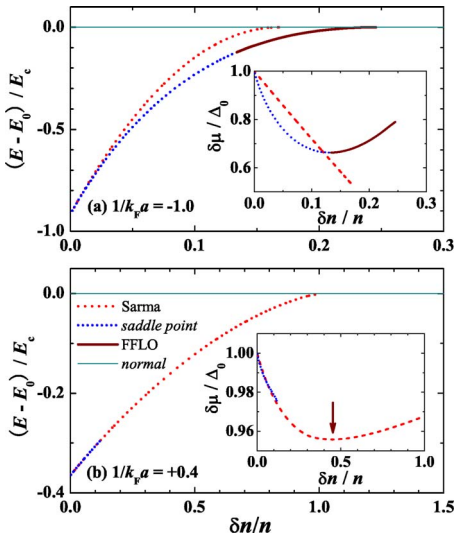


FIG. 4. (Color online) Comparison of energies of competing phases. Insets show the chemical potential difference as a function of polarization. The arrow in the inset of (b) indicates a position, above which the slope of the curve becomes positive.

*Fixed population imbalance*. In this case, the phase diagram is determined by minimizing $E = \Omega + \mu n + \delta\mu\,\delta n$. As shown in Fig. 4, now the spatially modulated saddle point phase and the FFLO phase are energetically preferable if they exist. Therefore, on the BCS side, with increasing imbalance the system goes from the saddle point state to the FFLO state, and finally turns into a normal gas [Fig. 4(a)]. As the interaction strengths increase, the FFLO state disappears and the saddle point phase also fades away, while the Sarma state starts to be supportive [Fig. 4(b)]. In the strong coupling BEC limit, the Sarma state becomes the only solution left.

The above discussion yields a phase diagram in the plane of interaction and polarization $\delta n/n$, as plotted in Fig. 5. It is topologically similar to the diagram in the $\eta - \delta\mu$ plane, except that the BCS pairing phase has now been replaced everywhere by the saddle point phase. However, it is important to point out that the saddle point phase (shadow regions in the figure), together with a sliver of the Sarma state, are intrinsically unstable towards phase separation, since the

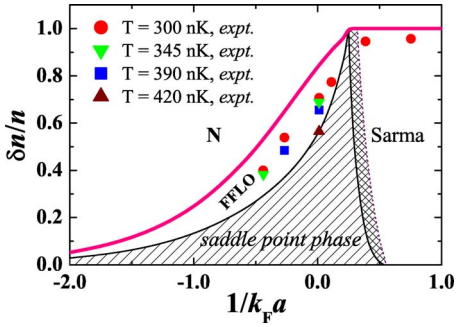


FIG. 5. (Color online) Interaction-porlarization phase diagram. The superfluid-to-normal transition boundary (thick line) is to be compared with the experimental data (symbols). The shadowed region is unstable against phase separation.

slope of the plot of $\delta\mu$ versus $\delta n$ for these phases is negative, as illustrated in the insets of Fig. 4. This is exactly the *precursor* for a spatially inhomogeneous mixed phase [6]. Around the crossover, our prediction for the appearance of the phase separation phase is consistent with the experimental observations [1,2].

In Fig. 5 we compare again the predicted boundary for the superfluid-to-normal transition with the experimental findings of critical polarization $(\delta n/n)_c$ [1]. The agreement seems to be qualitatively good. We note, however, that the most intriguing FFLO state is not identified experimentally. The window for the FFLO state in our phase diagram is sizable, but it may shrink rapidly with increasing temperature and an external trap as in experiments.

We conclude by discussing the possible effects of quantum pair fluctuations beyond mean field. Three remarks are in order concerning the $\eta-(\delta n/n)$ phase diagram. First, though within mean field the BCS state is strictly confined to the horizontal axis ($\delta n=0$), the inclusion of the pair fluctuations may accommodate a finite population imbalance. As a result, a narrow window for a uniform BCS superfluid opens close to the axis of $\delta n=0$ inside the saddle point phase. Secondly, in our mean-field theory the phase boundary for the mixed phase is determined indirectly from an instability analysis. It can also be fixed following the way shown in Ref. [6], i.e., by examining the energy of an incoherent mixture of some pure states. This alternative method requires consideration of pair fluctuations on the strong coupling BEC side. Finally, so far we restrict our analysis to the free space. With a finite trap one may instead solve the mean-field Bogoliubov–de Gennes equations or resort to the local density approximation [14]. The latter approach is particularly useful in order to take into account the pair fluctuations in the presence of traps. Details of these issues on quantum fluctuations will be presented elsewhere.

We acknowledge stimulating discussions with Professor P. D. Drummond. This work was supported by the Australian Research Council Center of Excellence and National Science Foundation of China Grant No. NSFC-10574080.

[1] M. W. Zwierlein *et al.*, Science **311**, 492 (2006).
[2] G. B. Partidge *et al.*, Science **311**, 503 (2006).
[3] P. Fulde and R. A. Ferrell, Phys. Rev. **135**, A550 (1964); A. I. Larkin and Y. N. Ovchinnikov, Zh. Eksp. Teor. Fiz. **47**, 1136 (1964) [Sov. Phys. JETP **20**, 762 (1965)]; T. Mizushima *et al.*, Phys. Rev. Lett. **94**, 060404 (2005).
[4] G. Sarma, J. Phys. Chem. Solids **24**, 1029 (1963); W. V. Liu and F. Wilczek, Phys. Rev. Lett. **90**, 047002 (2003).
[5] C.-H. Pao, S.-T. Wu, and S.-K. Yip, Phys. Rev. B **73**, 132506 (2006).
[6] P. F. Bedaque, H. Caldas, and G. Rupak, Phys. Rev. Lett. **91**, 247002 (2003).
[7] D. T. Son and M. A. Stephanov, e-print cond-mat/0507586.
[8] D. E. Sheehy and L. Radzihovsky, Phys. Rev. Lett. **96**, 060401 (2006).
[9] J. Carlson and S. Reddy, Phys. Rev. Lett. **95**, 060401 (2005).
[10] R. Casalbuoni and G. Nardulli, Rev. Mod. Phys. **76**, 263 (2004).
[11] L. He, M. Jin, and P. Zhang, e-print cond-mat/0601147.
[12] X.-J. Liu and H. Hu, Phys. Rev. A **72**, 063613 (2005).
[13] We assume the existence of a single **q** for FFLO states. The general case of multiple **q** can also be examined (see Ref. [10]).
[14] F. Chevy, Phys. Rev. Lett. **96**, 130401 (2006); W. Yi and L.-M. Duan, Phys. Rev. A **73**, 031604(R) (2006); T. N. De Silva and E. J. Mueller, e-print cond-mat/0601314; M. Haquea and H. T. C. Stoof, e-print cond-mat/0601321; P. Pieri and G. C. Strinati, e-print cond-mat/0512354; Z.-C. Gu, G. Warner, and F. Zhou, e-print cond-mat/0603091.